UNSUPERVISED WINTER WHEAT MAPPING BASED ON MULTI-SPECTRAL AND SYNTHETIC APERTURE RADAR OBSERVATIONS

H. Y. Li [1*], J. A. Lawrence [1], P. J. Mason [2], R. C. Ghail [3]

[1] Department of Civil and Environmental Engineering, Skempton Building, Imperial College London, South Kensington, London SW7 2AZ, UK – *hsuan-yi.li22@imperial.ac.uk;

[2] Department of Earth Science & Engineering, Imperial College London, Prince Consort Road, London SW7 2AZ, UK;

[3] Department of Earth Sciences, Queens Building 245, Royal Holloway, University of London Egham, Surrey TW20 0EX, UK

KEY WORDS: Unsupervised machine learning, hierarchical clustering, Dynamic Time Warping, Sentinel-1, Sentinel-2, wheat, agronomy.

ABSTRACT:

Annual meteorological variations and the impact of climate change in recent years impacted on agricultural production and distribution. Since wheat is a main food resource and the most widely grown crop in the world, it is essential to ensure the sustainability of its production. Therefore, accurate wheat mapping is essential for agricultural production forecasts. Multi-spectral satellite image analysis, including supervised machine learning (ML) methods, has been applied to wheat and other crop mapping, but such passive, optical imaging approaches are strongly influenced by weather conditions and cloud cover, whilst the supervised ML algorithms are highly reliant on manual labelling and ground control data. To avoid the limitation of weather and cloud, this research integrates Sentinel-1 Synthetic Aperture Radar (SAR) data with Sentinel-2 multi-spectral image products to achieve more reliable and accurate winter wheat mapping. Normalised Difference Vegetation Index (NDVI) retrieved from multi-spectral imagery and Sentinel-1's dual-polarisation radar signals, VV, VH, acquired in different time series, are used as key inputs to an unsupervised ML model based on Dynamic Time Warping (DTW) and hierarchical clustering to prevent time-consuming manual labelling. The chosen study area lies in Norfolk, UK. The result of winter wheat classification with NDVI time series data in this study reaches 72% accuracy, but the improved classification integrating NDVI, VH, VV and VH/VV values achieves 86% accuracy. Future research will focus on optimizing the ML model with multi data integration in addition additional research sites will test more complicated scenarios and multiple crop classification.

1. INTRODUCTION

1.1 Background

Wheat is one of the most important food resources and most widely grown crops in the world (Giraldo *et al.,* 2019). The international demand for wheat continues to grow both in the daily life of society and as a crop to feed livestock, but the effects of climate change in recent years impact on consistent wheat production (Langridge *et al.*, 2022). Accurate wheat mapping can ensure food production and further improve estimates of yield and biomass to maintain the agricultural sustainability of the crop ultimately contributing to global food security. Remote sensing observations provide low-cost strategies to methods of mapping any crops. Multi-spectral remote sensing observations combined with the simple Vegetation Index (VI) based linear regression and supervised ML methods are applied in wheat mapping. Random Forest (RF), a commonly used supervised ML method for wheat mapping, provides higher accuracy than simple VI-based linear regression (Hunt *et al*., 2019). In previous studies, winter wheat maps have been produced with analysis of various VIs, such as NDVI and Leaf Area Index (LAI), and multi-band reflections extracted from multi-spectral image products through RF (Zhang *et al.*, 2019; Mashonganyika *et al.*, 2021). However, cloud cover, poor weather conditions and cloud shadows reduce the number of usable multi-spectral images, and these limitations lead to mapping inaccuracies. To improve the accuracy of winter wheat mapping, SAR image products, which are reliable under all weather conditions have been integrated with the multi-spectral image products through the use of RF, LightGBM and LSTM (Mohite *et al.*, 2019; Luo et al., 2022; Parida et al., 2023). Since RF, LightGBM and LSTM are supervised ML methods which require plentiful ground truth data for training, these methods are time and labour intensive.

In this study, the proposed unsupervised ML method achieves winter wheat mapping by analysing Sentinel -1 and -2 time series data with observations of NDVI differences throughout the winter wheat phenology from previous studies (Wang *et al.*, 2021), as shown in Figure 1. The method does not require ground truth as the initial input can accurately identify areas of winter wheat.

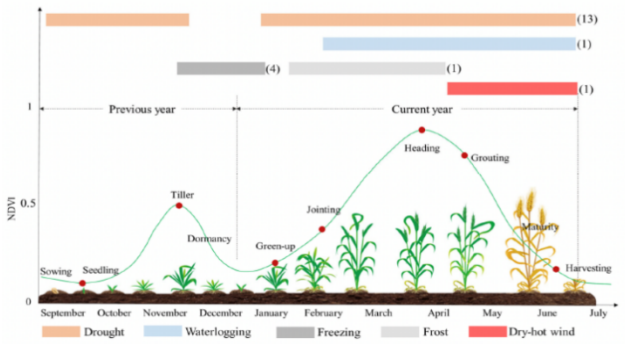

Figure 1. Normalized Difference Vegetation Index (NDVI) variation of winter wheat throughout the annual growth cycle (Wang *et al.*, 2021).

1.2 Aims and Objectives

This research combines two main objectives: (1) development of an unsupervised ML model for winter wheat mapping, and (2) improvement in winter wheat classification accuracy by integrating SAR with multi-spectral image products. This can reduce the impact of optical images with low quality on cloudy days and extend the application to data acquired at different dates and times. In addition, it solves the problem of the time related with supervised ML and the associated labour; the unsupervised ML model can be constructed without large amount of ground truths. The proposed method aims to provide an improved

unsupervised ML model for winter wheat mapping by integrating SAR with multi-spectral image products.

2. METHODOLODY

2.1 Unsupervised wheat mapping workflow

Figure 2 shows the workflow research methodology for the unsupervised ML model for wheat mapping using Earth Observation satellite imagery, Sentinel-1 and 2 image products. Sentinel-1 SAR image products are co-registered to Sentinel-2 multi-spectral images in UTM/WGS84 projection and resampled to a pixel size of 60 x 60 m. NDVI values from Sentinel-2 optical imagery and VV, VH and VH/VV SAR amplitude values from Sentinel-1 are extracted on a pixel-by-pixel basis and formed into time series. The 'distances' in the time series data of each pixel, in value and time, are calculated using DTW. Pixels are classified into five groups with four distance matrixes, NDVI, VV, VH and VH/VV through hierarchical clustering and the initial results are geo-referenced and exported as Geo Tiff files. By analysing the initial results, weights of NDVI, VV, VH and VH/VV are given as the input in the final ML model.

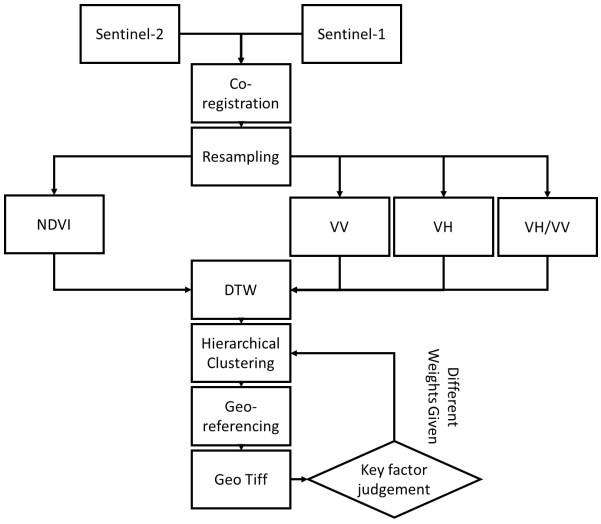

Figure 2. The workflow of this research.

2.2 Satellite imagery

SAR and multi-spectral images of the Norfolk area, with a sensing period between December 2019 to June 2020 were collected from Copernicus Open Access Hub of ESA (ESA, 2020). Sentinel-1 Level-1 Interferometric Wide (IW) Ground Range Detected (GRD) SAR image products and Sentinel-2 Level-2A multi-spectral image products referenced with UTM/WGS84 projection are applied in this research. Sentinel-1 Level-1 IW GRD SAR images applied in this study have 20 m in range and 22 m in azimuth, spatial resolution products with a 12 day repeat cycle involving dual polarisations, VV and VH backscattering measurements. Sentinel-2 Level-2A multi-spectral image products combine 13 spectral bands across the Coastal aerosol, Visible, Near Infra-Red (NIR), Water Vapor and Short-Wave Infra-Red (SWIR) spectrum, with a 5-day revisit time. Images depending on different spectral bands have Ground Sampling Distance (GSD) of 10 m, 20 m, or 60 m, as shown in Table 1. This research retrieves NDVI values in time series with 10 m resolution NIR and R band image products through equation (1).

Table 1. Sentinel-2 MSI sensor band specifications.

Band	Spectrum	Wavelength (nm)	Spatial Resolution (m)
B1	Coastal aerosol	433-453	60
B2	Blue	458-523	10
B3	Green	543-578	10
B4	Red	650-680	10
B5	Red edge	698-713	20
B6	Red edge	733-748	20
B7	Red edge	773-793	20
B8	NIR	785-900	10
B8A	Narrow NIR	855-875	20
B9	Water Vapor	935-955	60
B10	SWIR Cirrus	1360-1390	60
B11	SWIR 1	1565-1655	20
B12	SWIR2	2100-2280	20

$$NDVI = \frac{NIR - Red}{NIR + Red}, \quad (1)$$

where NIR = The reflection value of Near InfraRed Band.
Red = The reflection value of Red Band.

2.3 Dynamic Time Warping

Dynamic Time Warping (DTW) is a method to measure the similarity of data in two time sequences by calculating the 'distances' among discrete signals. Unlike the one-to-one traditional way of computing distances between two signals at the same time point, such as Euclidean, DTW is a one-to-many or many-to-one method to calculate distances among two or more signals at multiple time points in two time sequences, as shown in Figure 3. Thus, DTW is applied to analyse the similarity of the shapes of two or more time series data in the same time period.

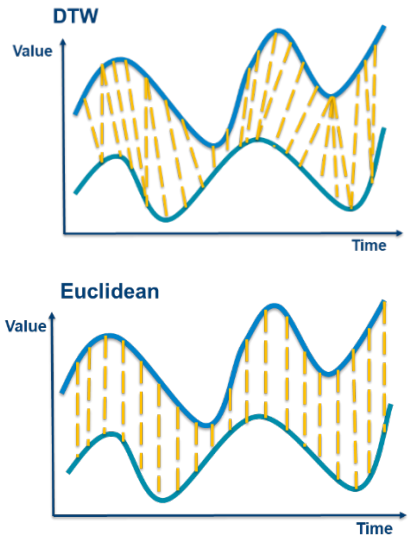

Figure 3. DTW calculates distances among signals at different time points, while Euclidean calculates distances among signals at the same time points.

The method extracts NDVI values from Sentinel-2 and the VH and VV measurements and VH/VV values from Sentinel-1 in the same time series from December 2019 to June 2020. Then the NDVI, VH, VV and VH/VV in each pixel is set into NDVI, VH, VV and VH/VV time series data. The distances between the NDVI, VH, VV and VH/VV time series data for each pixel are computed with DTW. The similarities among pixels, are then applied using a hierarchical clustering technique, which analyses by identifying the distances between the time series data in each pixel.

2.4 Hierarchical Clustering

Hierarchical clustering is an unsupervised ML method to compute the proximities among individuals and classify those into clusters. The clusters are merged into groups according to their similarities in steps. Each step merges similar clusters together and creates a layer in the tree-like diagram or dendrogram. Finally, all clusters are merged into one cluster and the completed dendrogram is formed. Within the dendrogram, the similarities among each cluster and individuals can be more easily visualised, as shown in Figure 4.

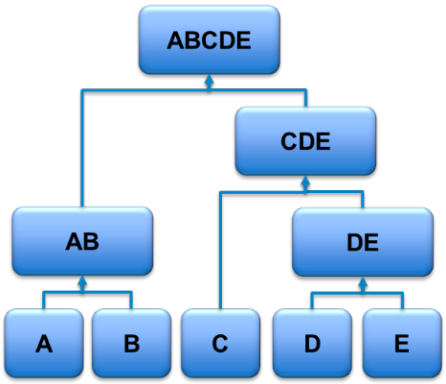

Figure 4. The concept of hierarchical clustering. The distances among five individuals, A, B, C, D and E, are calculated and the closest individuals, A and B, and D and E, are grouped together. The distances among groups, A and B, D and E, and the individual, C, are calculated. In the second layer, since C is closer to DE, thus C, D and E are gathered, and A and B still remain in the same group. The final layer gathers all individuals in the same group and the dendrogram of A, B, C, D, and E is formed.

The distance matrixes of NDVI, VH, VV and VH/VV, which are computed with the time series data in each pixel, are the inputs for the hierarchical clustering in this study. Each pixel is classified into five clusters with the distance matrixes. The number of clusters can be automatically defined with the hierarchical clustering ML model or limited with the manual settings. In this research, through the observations with NDVI, VV, VH and VH/VV values, the land cover is classified into five clusters, wheat, soil, urban, other vegetation and others.

2.5 Pixel Post-processing

Pixels are classified into five clusters with hierarchical clustering and the cluster number is assigned to each pixel. Numbered pixels are geo-referenced to UTM zone 30N/ WGS84 projection and exported as a Geo Tiff file.

Four types of Geo Tiff files are produced through four hierarchical clustering ML models with NDVI, VH, VV and VH/VV individually. In analysing four results, different weights are assigned to distance matrixes of NDVI, VV, VH and VH/VV. The weighted variables become new inputs for the final hierarchical clustering ML model to generate the integrated final improved results.

3. RESULTS

East Anglia, which comprises Norfolk, Suffolk and Cambridgeshire and Essex, is located in the east of England, UK and is considered Britain's 'breadbasket' and is a centre for horticulture, pig and poultry farming. Norfolk is ideal for horticultural farming methods with flat level fields, favourable climate and fertile soils. Norfolk has over 6,800 hectares of prime agricultural land and, within it, an of 600 x 600 m has been selected as the study area of this research, as shown in Figure 5.

The method extracts winter wheat areas from the Sentinel-1 and -2 time series data with the unsupervised hierarchical ML models. Four types of results are presented in Figures 6 and 7 to analyse given weights for the classification, these are based on:

(1) NDVI values from Sentinel-2;

(2) VH measurements from Sentinel-1;

(3) VV measurements from Sentinel-1; and

(4) VH/VV values from Sentinel-1.

Pixels within the study area are classified into five groups as shown in Figures 6 and 7, winter wheat is represented by green pixels, soil by orange pixels, urban areas by yellow pixels, and other classes are represented by red pixels.

These results are referenced and therefore validated against the Sentinel-2 Level 2A optical image and the crop classification result from the Rural Payments Agency (RPA), UK. The crop classification result provided by the RPA, UK was classified using RF with Sentinel -1 and 2 dataset.

Comparing the results from the RPA, UK, as shown in Figure 5 with the Sentinel-2 Level-2A optical image, the classification (1) and NDVI values from Sentinel-2(figure 6a) shows the best results. For winter wheat mapping, the accuracy is 72% with only two pixels are misclassified as the winter wheat area. This might be influenced by the boundary effect of the interpolation in resampling, which may obtain incorrect values at the boundary (Yaroslavsky, 2003).

In Figure 7a, the classification (2) with VH has a winter wheat mapping accuracy of 65%, but five pixels are misclassified as the winter wheat; in Figures 7b and 7c, The classification (3) with VV and the classification (4) with VH/VV do not accurately map the winter wheat mapping or clustering of the land cover, but still can represent the sensitivity of VV and VH/VV among pixels.

Comparing the classification (1) in Figure 6a and (2) in Figure 7a, the classification (1) with NDVI in Figure 6a is more accurate than the classification (2) with VH in Figure 7a. Thus, the improved ML model for the final result has NDVI as the key factor, VH as the sub dominant factor and VV and VH/VV as the supplementary factors determined by the dendrogram in Figure 6b. The improved winter wheat classification and the dendrogram of the ML (Figure 6b) model integrates NDVI, VH, VV and VH/VV. The result (5), as shown in Figure 6b, approaches 86 % accuracy in winter wheat mapping, which is an improves on result (1) in Figure 6a. The dendrograms for results (1) in Figure 6a and (5) in Figure 6b share a very similar grouping structure but slightly different in grouping of layers.

From the Sentinel-2 optical images, it can be seen that some parts of the hedgerows are being defined as the winter wheat field in the RPA, UK results (Figure 5b). However, in this study, the classifications of both (1) and (5), (Figure 6), show more accurate classification toward the boundary of the fields, the hedgerows

are not included in the winter wheat area. Since this study only focuses on the winter wheat and does not provide detailed analysis for other vegetation or landcover, the accuracy of landcover other than winter wheat fields are not determined.

(a)

(b)

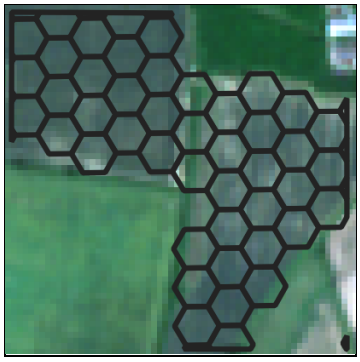

Figure 5. (a) The location of Norfolk in the UK. The yellow areas represent the 2020 winter wheat map in Norfolk. The red rectangular box shows the selected study area in this research. (b) Detailed view of the study area; the hexagons represent winter wheat areas generated from the RPA, UK. (Rural Payments Agency, UK, 2021)

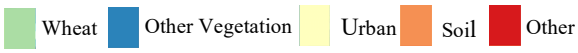

(a) NDVI only (1)

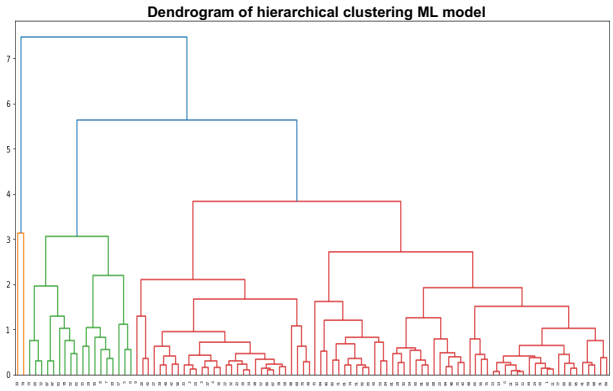

(b) NDVI+VV+VH+VH/VV (5)

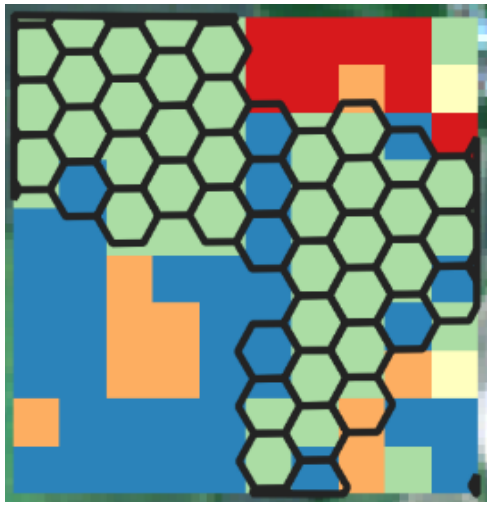

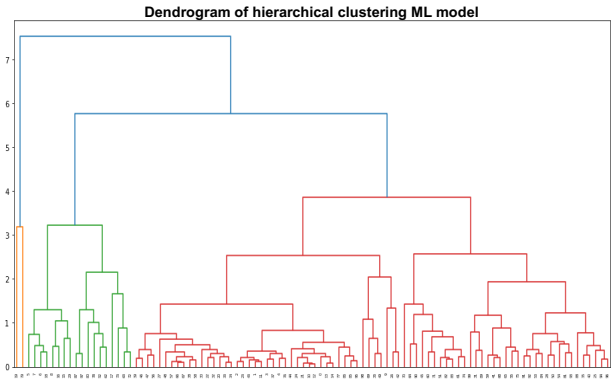

Figure 6. (a) The result generated using NDVI values and its dendrogram, with 72% accuracy. (b) The improved result (integrating NDVI, VV, VH, VH/VV values) and its dendrogram yielding 86% accuracy. In the maps, green pixels represent winter wheat areas.

(a) VH (2)

(b) VV (3)

(c) VH/VV (4)

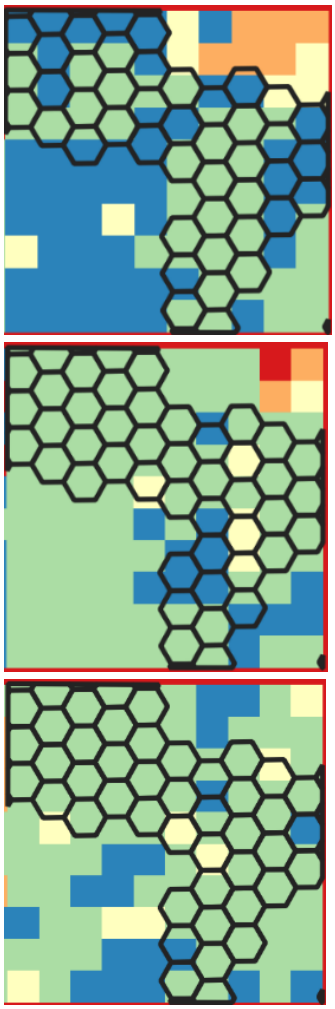

Figure 7. (a) The result with VH measurements. (b) The result with VV measurements. (c) The result with VH/VV values.

4. CONCLUSIONS

The proposed method establishes an unsupervised ML model based on freely available Earth Observation (EO) data from Sentinel-1 and -2 images, for improved winter wheat mapping. The main outcomes of this work are:

(1) The integration of SAR backscatter with a multi-spectral vegetation index improves the accuracy of winter wheat mapping, when compared with mapping from multi-spectral data alone.

(2) This research develops an unsupervised hierarchical ML model with DTW for winter wheat mapping. DTW precisely calculates the numerical distances among pixels in the time sequence, which reduces the computing time and increases the accuracy of clustering.

(3) Through the winter wheat maps generated with NDVI, VH, VV, VH/VV, this study analyses the sensitivity of NDVI, VH, VV and VH/VV values toward winter wheat. NDVI time series data is the dominant variable and VH is the second key variable, VV and VH/VV are the supplementary variables for winter wheat classification.

(4) The proposed unsupervised ML method, which requires zero ground truth provides an accurate winter wheat map as compared to the map produced by RPA, UK. The improved winter wheat map which integrates NDVI, VH, VV, VH/VV values show the best results, achieving an 86 % accuracy. which can be applied more broadly in other wheat crop areas.

5. FUTURE WORK

Future developments will focus on optimizing the unsupervised ML model for multiple crop type and vegetation classifications in the UK and beyond. The growth cycle of multiple crops will be analysed and more data types will be integrated in the future research. Three main future tasks have been identified as:

(1) Analysis of the phenology of multiple crop types to understand the conditions of the plants in various VIs and multi-band images and backscattered VV and VH polarisations.

(2) Testing of the proposed ML model at regional scales, adding complexity to further validate the results. Based on the tests, the ML model will be optimized and available for the multiple crop classifications.

(3) Integration of other complementary data types to improve the accuracy and precision of the proposed unsupervised ML model.

6. ACKNOWLEDGEMENTS

The authors acknowledge the support of the British Geotechnical Association (BGA) in the form of a BGA award, which enabled the first author to attend the International Society for Photogrammetry and Remote Sensing (ISPRS) Geospatial Week 2023.

REFERENCES

European Space Agency, 2020. Sentinel-1. https://sentinel.esa.int/web/sentinel/missions/sentinel-1.

European Space Agency, 2020. Sentinel-2. https://sentinel.esa.int/web/sentinel/missions/sentinel-2.

Giraldo, P., Benavente, E., Manzano-Agugliaro, F., Gimenez, E., 2019: Worldwide Research Trends on Wheat and Barley: A Bibliometric Comparative Analysis. *Agronomy*, 9(7), 352. doi.org/10.3390/agronomy9070352.

Hunt, M., Blackburn, G.A., Carrasco L., Redhead, J.W., Rowland, C.S., 2019: High resolution wheat yield mapping using Sentinel-2, *Remote Sensing of Environment*, 233, 111410. doi.org/10.1016/j.rse.2019.111410.

Langridge, P., Alaux, M., Almeida, N.F., Ammar, K., Baum, M., Bekkaoui, F., Bentley, A.R., Beres, B.L., Berger, B., Braun, H.-J., et al., 2022: Meeting the Challenges Facing Wheat Production: The Strategic Research Agenda of the Global Wheat Initiative. *Agronomy*, 12 (11), 2767. doi.org/10.3390/agronomy12112767.

Luo, Y., Zhang, Z., Cao, J., Zhang, L., Zhang, J., Han, J., Zhuang, H., Cheng, F., Tao, F., 2022: Accurately mapping global wheat production system using deep learning algorithms. *International Journal of Applied Earth Observation and Geoinformation*, 110, 102823. doi.org/10.1016/j.jag.2022.102823.

Mashonganyika, F., Mugiyo, H., Svotwa, E., Kutywayo, D., 2021: Mapping of Winter Wheat Using Sentinel-2 NDVI Data.

A Case of Mashonaland Central Province in Zimbabwe. *Front. Clim.*, 3, 715837. doi: 10.3389/fclim.2021.715837.

Mohite, J.D., Sawant, S.A., Rana, S., Pappula, S., 2019: WHEAT AREA MAPPING AND PHENOLOGY DETECTION USING SYNTHETIC APERTURE RADAR AND MULTI MULTI-SPECTRAL REMOTE SENSING OBSERVATIONS. *The International Archives of the Photogrammetry, Remote Sensing and Spatial Information Sciences*, XLII-3/W6, 123-127. doi.org/10.5194/isprs-archives-XLII-3-W6-123-2019.

Parida, B.R., Singh, S., 2023: Spatial mapping of winter wheat using C-band SAR (Sentinel-1A) data and yield prediction in Gorakhpur district, Uttar Pradesh (India). *Journal of Spatial Science*, 68(1), 91-106. doi.org/10.1080/14498596.2021.1896393.

Rural Payments Agency, 2021. Crop Map of England (CROME) 2020. https://www.data.gov.uk/dataset/be5d88c9-acfb-4052-bf6b-ee9a416cfe60/crop-map-of-england-crome-2020#licence-info.

Wang, S., Rao, Y., Chen, J., Liu, L., Wang, W., 2021: Adopting "Difference-in-Differences" Method to Monitor Crop Response to Agrometeorological Hazards with Satellite Data: A Case Study of Dry-Hot Wind. *Remote Sensing*, 13, 482. doi.org/10.3390/rs13030482.

Yaroslavsky, L., 2003: Boundary Effect Free and Adaptive Discrete Signal Sinc-Interpolation Algorithms for Signal and Image Resampling: Erratum. *Applied optics*, 42(20), 4166-4175. doi.org/10.1364/AO.42.004166.

Zhang, D., Fang, S., She, B., Zhang, H., Jin, N., Xia, H., Yang, Y., Ding, Y., 2019: Winter Wheat Mapping Based on Sentinel-2 Data in Heterogeneous Planting Conditions. *Remote Sensing*, 11, 2647. doi.org/10.3390/rs11222647.